

# High-power, high-brightness solar laser approach for renewable Mg recovery from MgO

Joana Almeida and Dawei Liang\*

CEFITEC, Departamento de Física, FCT, Universidade Nova de Lisboa, 2829-516 Campus de Caparica, Portugal

## ABSTRACT

Hydrogen and heat energy from the reaction of magnesium with water can be used for engines and fuel cells. However, at least 4000 K is necessary for magnesium oxide reduction. Ultra high brightness solar-pumped lasers become essential to make this renewable process technology efficient and economically competitive. 2.3 mg/kJ solar laser - induced magnesium production efficiency has been achieved by T. Yabe et al., in 2012, by focusing a 53 W solar laser beam on a mixture of MgO with Si as reducing agent. This result is however far from the 12.1 mg/kJ attained with 2 kW/mm<sup>2</sup> CO<sub>2</sub> laser beam. To improve substantially the solar laser - induced Mg production efficiency, a simple high-power, high brightness Nd:YAG solar laser pumping approach is proposed. The solar radiation is both collected and concentrated by four Fresnel lenses, and redirected towards a Nd:YAG laser head by four plane folding mirrors. A fused-silica secondary concentrator is used to compress the highly concentrated solar radiation to a laser rod. Optimum pumping conditions and laser resonator parameters are found through ZEMAX<sup>®</sup> and LASCAD<sup>®</sup> numerical analysis. High-record solar laser beam brightness figure of merit - defined as the ratio between laser power and the product of  $M_x^2$  and  $M_y^2$  - of 10.5 W is numerically achieved, being 5.5 times higher than the previous record and about 1600 times more than that of the most powerful Nd:YAG solar laser. 8340 W/mm<sup>2</sup> is numerically achieved at its focal region, which can quadruple the magnesium production efficiency with clean energy.

**Keywords:** Solar-pumped laser, high-power, high-brightness, magnesium, Fresnel lens, Nd:YAG, laser cavity, MgO

## 1. INTRODUCTION

Solar lasers have a large potential for many applications, e.g. high-temperature materials processing, renewable, free space laser communications, space to earth power transmission and so on. They are necessary in remote locations where other forms of energy are scarce and sunlight is abundant. Compared to electrically powered lasers, solar-pumped solid-state lasers are much simpler and more reliable due to the complete elimination of the electrical power generation and conditioning equipments, offering the prospect of a drastic reduction in the cost of coherent optical radiation for high average power applications.

The renewable magnesium (Mg) - hydrogen (H<sub>2</sub>) cycle is also a very interesting topic for solar laser research. There is a huge Mg resource of  $1.8 \times 10^{15}$  tons in the ocean [1]. Large amounts of heat and H<sub>2</sub> are given off from the reaction of Mg with water (H<sub>2</sub>O), which can be used in fuel cell vehicles applications. Since laser radiation can be focused to a small spot, a very high temperature exceeding 4000 K, needed for MgO deoxidization, can be easily obtained and the MgO residue can hence be refined back to Mg by laser radiation [1, 2]. High-power solar-pumped lasers with excellent beam quality are essential for the success of this application. 2.3 mg/kJ solar laser - induced magnesium production efficiency has been achieved by T. Yabe et al., in 2012, by focusing a 53 W solar laser beam on a mixture of MgO with Si as reducing agent [3]. This result is however far from the 12.1 mg/kJ attained with 2 kW/mm<sup>2</sup> CO<sub>2</sub> laser beam [4].

Since the first report of “A sun-pumped cw one-watt laser” in 1966 [5], optical and laser material advances have continued to improve solar-pumped laser performance. Despite the small overlap between the Nd:YAG absorption spectrum and the solar spectrum, Nd:YAG has been demonstrated as the best material under solar pumping because of its superior characteristic on thermal conductivity, high quantum efficiency and mechanical strength compared to other host materials [5-14]. Significant solar laser collection efficiencies have been achieved by end-pumping small diameter

Nd:YAG single-crystal rods [10-12]. The most recent end-pumped Nd:YAG solar laser has produced the record collection efficiency of 30.0 W/m<sup>2</sup> with a large diameter Nd:YAG rod [12]. However, very large  $M_x^2 = M_y^2 = 137$  factors have also been reported, resulting in a dismal brightness figure of merit - defined as the ratio between laser power and the product of  $M_x^2$  and  $M_y^2$  - of only 0.0064 W. Although the most efficient laser systems have end-pumping approaches, side-pumping configurations are very suitable for laser power scaling. This allows a more uniform pump absorption profile along the laser medium. The associated thermal loading problems can hence be reduced. Besides, the free access to both rod ends permits the optimization of more laser resonator parameters, improving largely the laser beam quality. Therefore, its brightness figure of merit can be higher than that of end-pumping approaches. 0.29 W solar laser beam brightness figure of merit has been achieved in 2011, by side-pumping a 4 mm Nd:YAG rod through the heliostat-parabolic mirror system in PROMES-CNRS [13]. This has remained as a record-high value until most recently, 1.9 W solar laser beam brightness figure of merit has been reported by side-pumping a 3 mm Nd:YAG rod [14]. This result has surpassed the previous record value by 6.6 times, with 2.3 W solar laser power operating in the lowest mode possible (TEM<sub>00</sub>).

To improve significantly the present-day solar laser beam brightness, an alternative solar collection and concentration design using Fresnel lenses is here proposed for application in the renewable Mg recovery from MgO. Incoming solar radiation is firstly concentrated by the four circular Fresnel lenses of 1 m<sup>2</sup> collection area, and then is redirected towards a common focal zone by four plane folding mirrors. A secondary concentrator composed of four semi-cylindrical fused silica lenses further compresses the concentrated solar light into a Nd:YAG single-crystal rod. Water is used as coolant to ensure both the efficient removal of the generated heat and also the light coupling from the lenses to the laser rod. Optimum pumping conditions and laser resonator parameters are found through ZEMAX<sup>®</sup> and LASCAD<sup>®</sup> numerical analysis, respectively. The proposed solar laser scheme allows both an efficient and uniform pumping to the laser rod. On one hand, maximum multimode solar laser power of 78.4 W is numerically achieved for a 7.5 mm diameter, 30 mm length Nd:YAG rod, corresponding to high collection efficiency of 19.6 W/mm<sup>2</sup> for side-pumped Nd:YAG solar laser. On the other hand, record high brightness figure of merit of 10.5 W is numerically achieved for a 5 mm diameter, 30 mm length Nd:YAG rod. This value is 5.5 times more than the record brightness figure of merit with TEM<sub>00</sub> mode Nd:YAG solar laser.

## 2. FRESNEL LENS-FOLDING MIRROR SOLAR ENERGY COLLECTION AND CONCENTRATION SYSTEM

The proposed solar laser side-pumping approach in Figure 1 is formed by a combination of four circular Fresnel lenses (F<sub>1</sub>-F<sub>4</sub>), which both collect and concentrate the solar radiation, and four elliptical plane mirrors (M<sub>1</sub>-M<sub>4</sub>) that redirect the concentrated solar radiation towards the laser head, located in the focal zone.

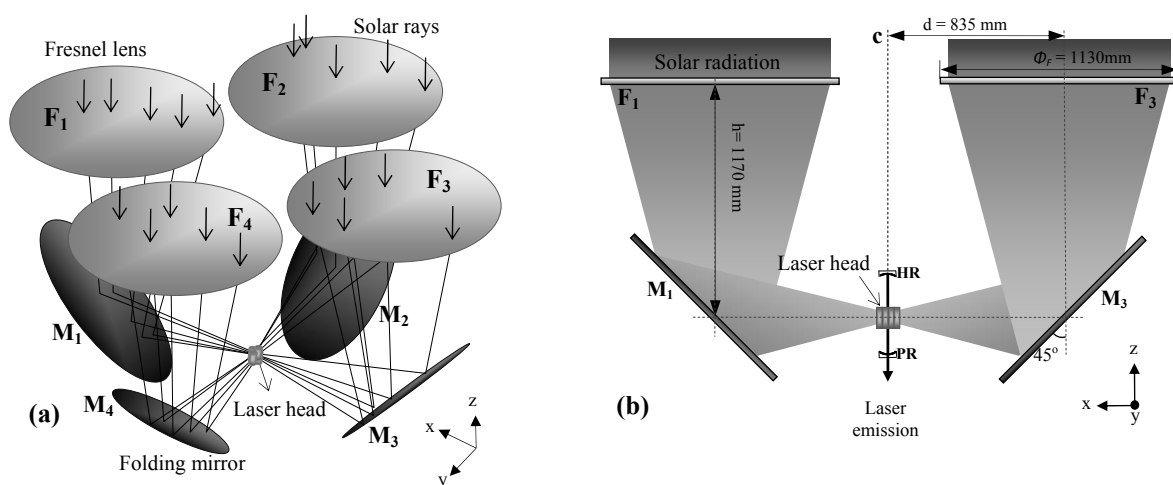


Figure 1. (a) Four Fresnel lens - folding mirror solar laser side-pumping approach. (b) Solar light collection and concentration in x-z plane.

Each Fresnel lens has  $1 \text{ m}^2$  area, which gives  $4 \text{ m}^2$  of total solar collection area. The Fresnel lenses have 2 m focal length and are coplanar in z-axis with  $d = 835 \text{ mm}$  spacing from the center of each Fresnel lens to their common optical center  $c$ , which is located  $h = 1170 \text{ mm}$  above the center of the laser head as shown in Fig. 1(b). Each folding mirror is placed below its respectively Fresnel lens, with a  $45^\circ$  inclination angle in relation to their common optical axis. Solar tracking can be achieved by mounting the whole laser system onto a two axis-heliostat that follows the Sun continuously in direct tracking mode. The two stepper motors of the solar tracker are controlled by both an electronic control unit with Global Positioning System (GPS) guidance for quick solar orientation with  $1.0^\circ$  accuracy and a photo sensing unit for accurate tracking with  $0.1^\circ$  accuracy.

### 3. FUSED SILICA SECONDARY CONCENTRATOR

The highly concentrated solar radiation from the Fresnel lens - folding mirror system is further compressed to the Nd:YAG laser rod through a set of four fused silica lenses with semi-cylindrical shape, as shown in Figure 2.

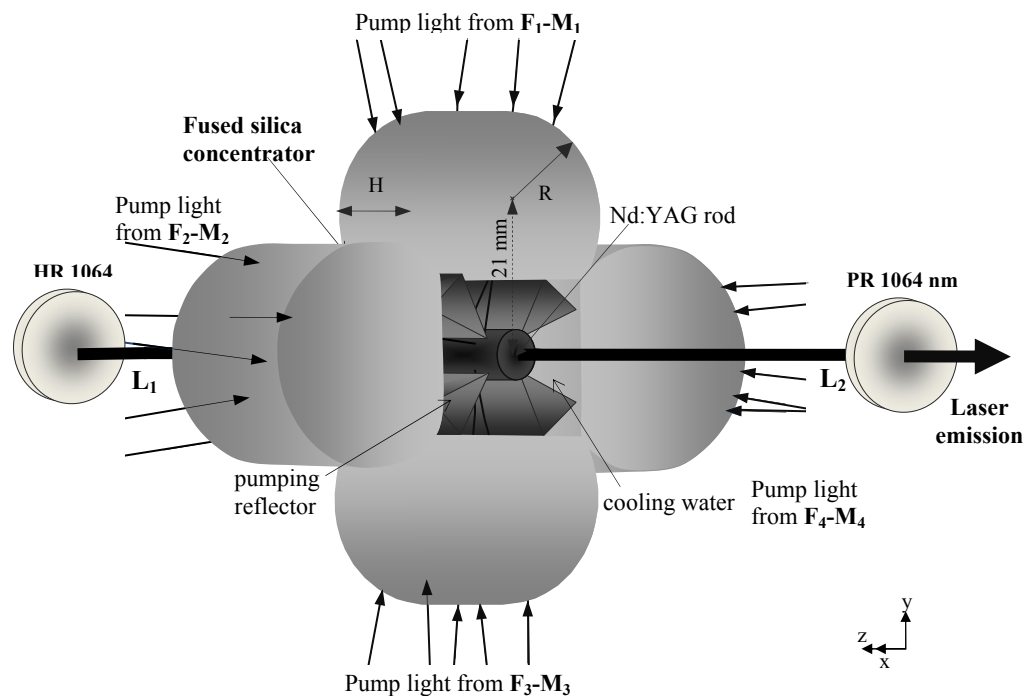


Figure 2. Laser head with fused silica secondary concentrators.

Fused silica is an ideal optical material for Nd:YAG laser pumping, since it is transparent over the Nd:YAG absorption spectrum. It has a high softening point and is resistant to scratching and thermal shock which also makes it very suitable for ultra-high power solar pumping. High optical quality fused silica concentrators (99.999%) can be manufactured by optical machining and polishing [15]. Each semi-cylindrical lens has  $R = 18 \text{ mm}$  curvature radius,  $H = 22 \text{ mm}$  height and its center is positioned  $21 \text{ mm}$  away from the central axis of the Nd:YAG rod of  $30 \text{ mm}$  length. The semi-cylindrical shape of the fused silica lenses allows an efficient and uniform pumping to the laser rod, which is cooled by cooling water. The maximum contact between the coolant and the active medium ensures the efficient removal of the generated heat. Inside the cooling channel, four V-shaped reflectors are evenly mounted around the laser rod to redirect some pump rays, which would otherwise miss the rod, to it. Both end faces of the Nd:YAG rod are  $1064 \text{ nm}$  anti reflection (AR) coated. The laser resonant cavity is formed by two opposing mirrors, one is  $1064 \text{ nm}$  high reflection (HR) coated while the other is  $1064 \text{ nm}$  partial reflection (PR) coated, as indicated in Figure 2.

#### 4. NUMERICAL ANALYSIS OF THE ND:YAG SOLAR LASER PERFORMANCES

The optical parameters of the proposed solar-pumping scheme are optimized through ZEMAX<sup>®</sup> non-sequential ray-tracing. The standard solar spectrum for one-and-a-half air mass (AM1.5) [16] is used as the reference data for consulting the spectral irradiance ( $\text{W}/\text{m}^2/\text{nm}$ ) at each wavelength. The terrestrial solar irradiance of  $950 \text{ W}/\text{m}^2$  is considered in ZEMAX<sup>®</sup> software. The effective pump power of the light source takes into account the 16% overlap between the absorption spectrum of the Nd:YAG medium and the solar spectrum [17]. The apparent half-angle of  $0.27^\circ$  subtended by the sun is also considered in the analysis. The absorption spectrum of Polymethyl Methacrylate (PMMA), fused silica and water materials are included in ZEMAX<sup>®</sup> numerical data to account for absorption losses.

For 1.1 at%  $\text{Nd}^{3+}$ -doped YAG single-crystal medium, 22 absorption peaks are defined in ZEMAX<sup>®</sup> numerical data. All the peak wavelengths and their respective absorption coefficients are added to the glass catalogue in ZEMAX<sup>®</sup> software. Solar irradiance values for the above-mentioned 22 peak absorption wavelengths could be consulted from the standard solar spectra for AM1.5 and saved as source wavelength data. During ray-tracing, the active medium is divided into a total of 18000 zones. The path length in each zone is found. With this value and the effective absorption coefficient, the absorbed power within the laser medium can be calculated by summing up the absorbed pump radiation of all zones. The absorbed pump flux data from the ZEMAX<sup>®</sup> analysis is then processed by LASCAD<sup>®</sup> software to study the laser beam parameters and quantify the thermal effects applied in the active medium. Figure 3 gives both the absorbed pump power and absorbed pump flux results, obtained through ZEMAX<sup>®</sup> analysis, for the 30 mm length Nd:YAG rods of different diameters. As observed in Figure 3, the absorbed pump power increases with larger diameter rods. On the contrary, the absorbed pump flux within the Nd:YAG mediums becomes smaller with larger diameter rods.

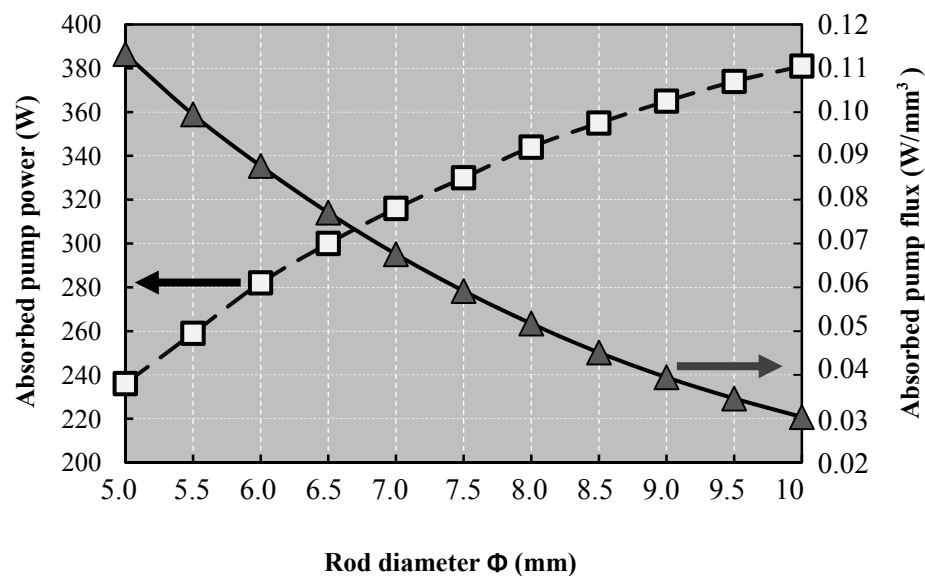


Figure 3. Absorbed pump power (primary axis) and absorbed pump flux (secondary axis) for the Nd:YAG rods of different diameter.

In LASCAD<sup>®</sup> analysis, the optical resonator is comprised of two opposing parallel mirrors at right angles to the axis of the active medium. The amount of feedback is determined by the reflectivity of the PR mirrors. One end mirror is high reflection coated (HR, 99.98%). The output coupler is partial reflection coated (PR) with reflectivity variable between 90 - 99%, according to different laser medium diameters. Figure 4 presents the maximum multimode solar laser power numerically attained with the different Nd:YAG rod diameters.

Maximum multimode laser power of 78.4 W is numerically found for the  $\Phi = 7.5 \text{ mm}$  Nd:YAG rod, resulting in high collection efficiency of  $19.6 \text{ W}/\text{m}^2$  for side-pumping configuration. When pumping larger diameter rods, the multimode laser power starts to decrease, despite the increased absorbed pump power verified in Figure 4. This behaviour can be explained by the drop of the absorbed pump flux within larger diameter rods.

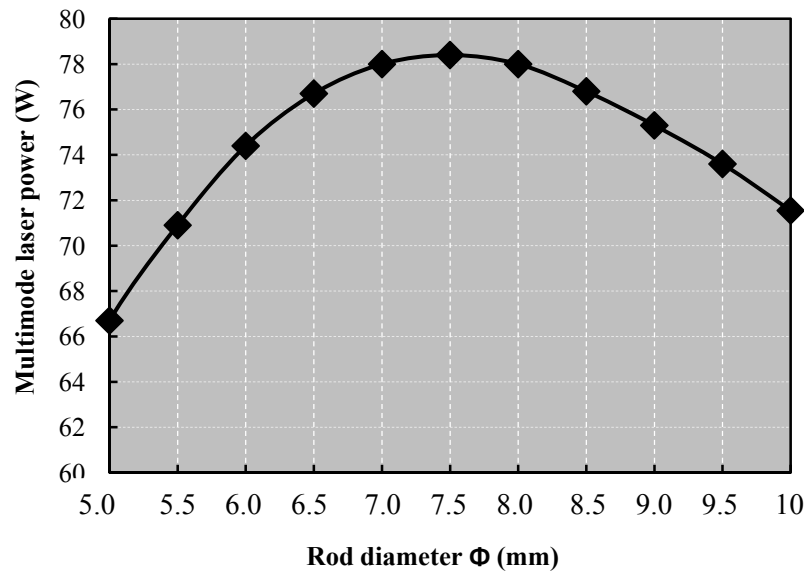


Figure 4. Maximum multimode solar laser power for the Nd:YAG rods of different diameters.

Pumping smaller diameter rods mean high absorbed pump flux and causes therefore the reduction in its thermal focal length in LASCAD© analysis. However, the laser beam quality is improved, since high-order resonator modes are suppressed due to larger diffraction losses. Table 1 compares the solar laser beam performances of the  $\Phi = 5.0$  mm and  $\Phi = 7.5$  mm rods. The asymmetric optical resonator with - 5 m radius of curvature (RoC) is found to be the best configuration for achieving low laser beam divergence. The laser cavity in Figure 6 with the - 5 m RoC rear mirror (HR 99.8 %) positioned at  $L_1 = 440$  mm and the - 5 m RoC output mirror (PR 90 %) positioned at  $L_2 = 50$  mm offers the best solar laser beam performance for the  $\Phi = 5$  mm Nd:YAG rod in LASCAD© analysis.  $M_x^2 = M_y^2 = 2.5$  beam quality factors are found in this case, resulting in high brightness figure of merit of 10.5 W, as shown in Table 1. This value is 5.5 times higher than the record brightness figure of merit for Nd:YAG TEM<sub>00</sub> solar laser [14] and about 1600 times than that of the most powerful Nd:YAG solar laser [12]. Although more laser output power is numerically attained for the  $\Phi = 7.5$  mm rod, this come at the expense of larger  $M_x^2 = 3.7$ ,  $M_y^2 = 3.8$  factors and consequently a lower brightness figure of merit of 5.6 W. Still, this value is almost 3 times greater than the record solar laser beam brightness figure of merit.

Table 1. Solar laser beam performance for the  $\Phi = 5$  mm and  $\Phi = 7.5$  mm Nd:YAG rods.

Rod diameter $\Phi$	5 mm	7.5 mm
<b>Resonator configuration</b>	Concave - concave	Concave - concave
Mirror radius of curvature (RoC)		
Rear	- 5 m	-5 m
Output	- 5 m	-5 m
Resonator length		
$L_1$	440 mm	685 mm
$L_2$	50 mm	50 mm
<b><math>M_x^2 / M_y^2</math> factors</b>	2.5 / 2.5	3.7 / 3.8
<b>Brightness figure of merit</b>	10.5 W	5.6 W

The grey-scale absorbed pump flux distribution within both the central and longitudinal cross-sections of the  $\Phi = 5$  mm Nd:YAG rod are shown in Figure 5. Black color means near maximum pump absorption, whereas white means little or no absorption. When the absorption profile is centrally peaked, the temperature on the axis increases further, resulting in stronger thermal lensing at the center, higher-order aberrations at the periphery, and larger stress in the laser rod compared with those of uniform excitation [18]. Consequently, to achieve high laser beam brightness, we should start with a low power deposition at the center of the medium, as shown in Figure 5, which can be easily achieved by the single-crystal Nd:YAG rod pumped through the proposed side-pumping solar laser scheme. Uniform pumping along the laser rod is also observed, hindering the creation of hot spots within the crystal. This can largely reduce the thermal lensing problems.

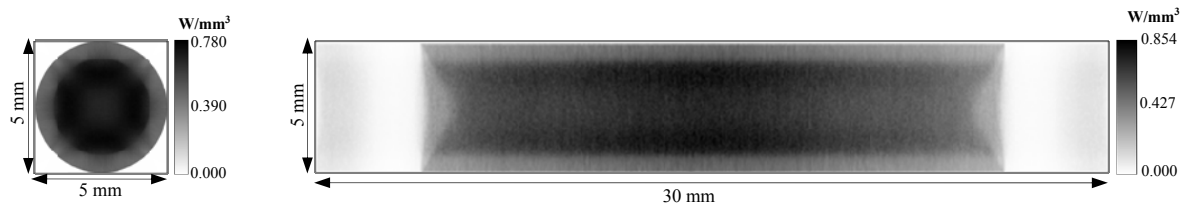


Figure 5. Absorbed pump flux distributions along both the central and longitudinal cross-sections of the  $\Phi = 5$  mm Nd:YAG rod.

For the  $\Phi = 5$  mm solar laser beam with low divergence, it is possible to attain less than  $50 \mu\text{m}$  diameter spot at the focal zone of a focusing lens with 40 mm focal length, as shown in Figure 6. About  $8340 \text{ W/mm}^2$  peak intensity can hence be achieved, which is more than 4 times the  $2000 \text{ W/mm}^2$   $\text{CO}_2$  laser flux for magnesium production.

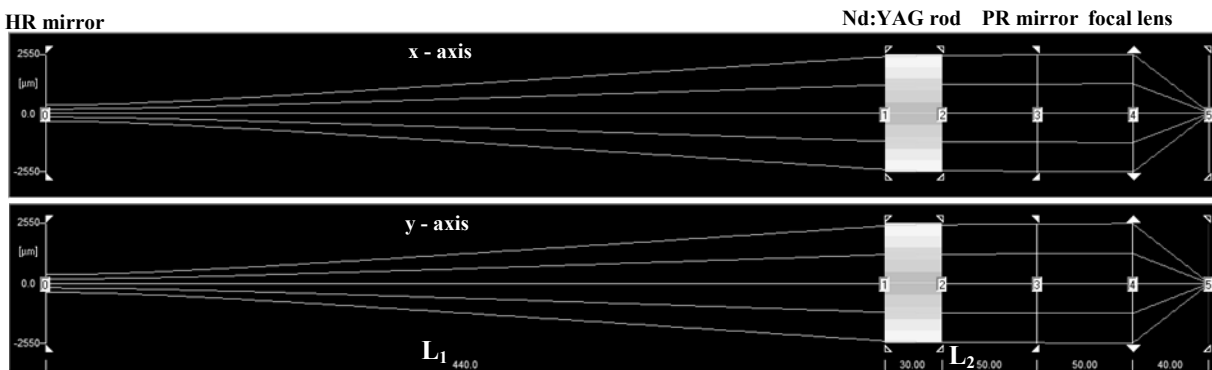


Figure 6. Asymmetrical laser resonator for the best solar laser performance with  $\Phi = 5$  mm Nd:YAG rod.

## 5. CONCLUSIONS

The alternative side-pumping approach is composed of the four circular Fresnel lens, four plane folding mirrors, the common secondary concentrator with four semi-cylindrical lenses and the V-shaped reflectors along the cooling channel where relies the Nd:YAG laser rod. This unique combination allows both an efficient and uniform pumping to the laser rod. Optimum optical pumping conditions are found through ZEMAX<sup>®</sup> software. Optimized laser resonator parameters are found through LASCAD<sup>®</sup> numerical analysis, by testing various Nd:YAG laser rods of different diameters within different resonator configurations. On one hand, high order multimode solar laser power of 78.4 W is numerically attained for the 7.5 mm diameter, 30 mm length Nd:YAG rod, leading to high collection efficiency of  $19.6 \text{ W/m}^2$  for side-pumped Nd:YAG laser. On the other hand, by adopting the large asymmetric concave-concave resonator configuration and the smaller diameter rod, 10.5 W solar laser beam brightness is numerically obtained, being 5.5 times more than the record value for Nd:YAG solar laser. The magnesium production efficiency with clean energy can hence be largely enhanced with the proposed side-pumped solar laser approach.

## ACKNOWLEDGMENTS

This research project PTDC/FIS/122420/2010 was funded by the Science and Technology Foundation of Portuguese Ministry of Science Technology and Higher Education (FCT-MCTES).

## REFERENCES

- [1] Yabe, T., Uchida, S., Ikuta, K., Yoshida, K., Baasandash, C., Mohamed, M. S., Sakurai, Y., Ogata, Y., Tuji, M., Mori, Y., Satoh, Y., Ohkubo, T., Murahara, M., Ikesue, A., Nakatsuka, M., Saiki, T., Motokoshi, S., and Yamanaka, C., "Demonstrated fossil-fuel-free energy cycle using magnesium and laser," *Appl. Phys. Lett.* 89, 261107 (2006).
- [2] Yabe, T., Suzuki, Y. and Satoh, Y., "Working prototype of magnesium batteries for cell phone and cars and magnesium recycling by lasers for renewable energy cycle," *Renewable Energy and Power Quality Journal (RE&PQJ)* ISSN 2172-038, No. 12, 2014.
- [3] Yabe, T., Tomomassa, O., Hung, D. T., Hiroki, K., Junichi, N. and Kouta, O., [Magnesium Technology], John Wiley & Sons, Inc., Hoboken, New Jersey, 55-58 (2012).
- [4] Liao, S. H., Yabe, T., "Laser-induced Mg production from magnesium oxide using Si-based agents and Si-based agents recycling," *J. Appl. Phys.* 109, 013103-9 (2011).
- [5] Young, C. G., "A sun pumped cw one-watt laser," *Appl. Opt.* 5(6), 993-997 (1966).
- [6] Weksler, M. and Shwartz, J., "Solar-pumped solid-state lasers," *IEEE J. Quantum Electron.* 24(6), 1222-1228 (1988).
- [7] Arashi, H., Oka, Y., Sasahara, N., Kaimai, A. and Ishigame, M., "A solar-pumped cw 18 W Nd:YAG laser," *Jpn. J. Appl. Phys.* 23 (8), 1051-1053 (1984).
- [8] Benmair, R. M. J., Kagan, J., Kalisky, Y., Noter, Y., Oron, M., Shimony, Y. and Yogev, A., "Solar-pumped Er, Tm, Ho: YAG laser," *Opt. Lett.* 15 (1), 36-38 (1990).
- [9] Lando, M., Kagan, J., Linyekin, B. and Dobrusin, V., "A solar pumped Nd:YAG laser in the high collection efficiency regime," *Opt. Commun.* 222(1-6), 371-381 (2003).
- [10] Almeida, J., Liang, D., Guillot, E. and Abdel-Hadi, Y., "A 40 W cw Nd:YAG solar laser pumped through a heliostat: a parabolic mirror system," *Laser Phys.* 23(6), 065801-6 (2013).
- [11] Liang, D. and Almeida, J., "Highly efficient solar pumped Nd:YAG laser," *Opt. Express* 19(27), 26399-26405 (2011).
- [12] Dinh, T. H., Ohkubo, T., Yabe, T. and Kuboyama, H., "120 watt continuous wave solar-pumped laser with a liquid light-guide lens and a Nd:YAG rod," *Opt. Lett.* 37(13), 2670-2672 (2012).
- [13] Almeida, J., Liang, D. and Guillot, E., "Improvement in solar-pumped Nd:YAG laser beam brightness," *Opt. Laser Technol.* 44(7), 2115-2119 (2012).
- [14] D. Liang, and J. Almeida, "Solar-pumped TEM<sub>00</sub> mode Nd:YAG laser," *Opt. Express* 21(21), 25107-25112 (2013).
- [15] Bernardes, P. H., and Liang, D., "Solid-state laser pumping by light-guides," *Appl. Opt.* 45(16), 3811-3816 (2006).
- [16] ASTM Standard G173 (2012).
- [17] Zhao, B., Zhao, C., He, J. and Yang, S., "The Study of Active Medium for Solar-Pumped Solid-State Lasers," *Acta Opt. Sin.* 2007(10), 1-9 (2006).
- [18] Brand, T., "Compact 170-W continuous-wave diode-pumped Nd:YAG rod laser with a cusp-shaped reflector," *Opt. Lett.* 20(17), 1776-1778 (1995).